Carbohydrate Polymers 111 (2014) 477–484

Contents lists available at ScienceDirect

Carbohydrate Polymers

journal homepage: www.elsevier.com/locate/carbpol

Sodium cobalt hexacyanoferrate encapsulated in alginate vesicle with CNT for both cesium and strontium removal

Adavan Kiliyankil Vipin*, Sun Ling, Bunshi Fugetsu

Graduate School of Environmental and Earth Science, Hokkaido University Kita-Ku, Kita-10, Nishi-5, Sapporo 060-0810, Japan

ARTICLE INFO

Article history:
Received 23 January 2014
Received in revised form 11 March 2014
Accepted 7 April 2014
Available online 21 April 2014

Keywords:
Cesium
Strontium
Sodium cobalthexacyanoferrate
Alginate
Carbon nanotubes
Adsorption

ABSTRACT

Sodium cobalt hexacyanoferrate (CoFC)-encapsulating alginate beads reinforced with highly dispersed multiwalled carbon nanotubes were prepared for the aqueous removal of cesium and strontium ions. Carbon nanotubes enhanced the effective surface area, encapsulation ability and adsorption capacity of beads. Equilibrium and kinetic studies were conducted with different mathematical models. The goodness of mathematical fitting of experimental data on the adsorption isotherm model was in the order Langmuir higher than Freundlich. The maximum Cs^+/Sr^{2+} adsorption capacity of beads modified with carbon nanotubes were 133/72 mg/g and that of beads without carbon nanotubes were 121/70 mg/g. Similarly in kinetic models pseudo-second-order gave better fitting than pseudo-first-order. The performance of beads was consistent in a wide range of pH as well as in high ionic competitions. The fixed bed adsorption column analysis indicated that beads can be used for large scale treatment of cesium and strontium contaminated water.

1. Introduction

Cesium-137 and strontium-90 are the principle medium lived fission products have half-lives of 30.17 and 28.8 years respectively (Todd et al., 2004) Nuclear weapon testing, uncontrolled discharge of waste effluents from nuclear reactors and nuclear fuel reprocessing, and accidental release are the major routes by which radioactive cesium and strontium have been introducing into the environment (Avery, 1996). They are highly hazardous materials as they can contaminate our natural resources such as water, soil, and air also enter the food chain through plants and ultimately incorporate into animals and human beings (Taj, Muhammad, Chaudhry, & Mazhar, 2011). Therefore, simultaneous removal of these dangerous radionuclides is highly desired. There are large numbers of technologies have been studied and many of them are capable of separating cesium and/or strontium under certain conditions only (Todd et al., 2004). However, there are only a handful of technologies that have been developed to the stage where they are ready for testing in prototypic equipment and processes. Separation techniques fall into two main categories, which are solvent extraction and ion exchange. Out of these techniques ion exchange is the most simple, economic and effective technique for dilute solutions (El-Kamash, 2008).

Sparingly soluble metal ferrocyanide, are known as an excellent scavenger of cesium, often used for the removal of radioactive cesium from nuclear waste solutions (Ishihara et al., 2011). Over the past four decades a wide variety of hexacyanoferrate(II) complexes of alkali and transition metal were prepared (Lehto, Harjula, & Wallace, 1987). From the insights of their structure and ion exchange properties, most of them are highly selective ion exchanger for cesium (Nilchi, Malek, Maragheh, & Khanchi, 2003). Sodium cobalt hexacyanoferrate is one of the novel materials known to be highly selective for cesium adsorption from aqueous waste (Mardan, Ajaz, Mehmood, Raza, & Ghaffar, 1999). However, it is unfeasible to use sodium cobalt hexacyanoferrate directly into water because the small particle size, also low permeability made this application in fixed-bed columns impractical. We selected alginate as a good immobilizer as well as a promising divalent adsorbent. Alginate is non-toxic, has high viscosity and molecular weight ranging from several to hundred thousand. They are widely distributed in organisms such as seaweeds and bacteria. Simultaneous binding of divalent cations such as Ca^{2+} or Ba^{2+} to different chains of α-L-guluronate units of alginate monomer to form stable biodegradable gel. The chains form (a structure resembling an "egg box") electronegative cavities capable of binding divalent cations via ionic interactions (Fundueanu, Nastruzzi, Carpov, Desbrieres, & Rinaudo, 1999; Lin, Fugetsu, Terui, & Tanaka, 2005; Papageorgiou,

* Corresponding author. Tel.: +81 117069235.
E-mail address: vipinak@ees.hokudai.ac.jp (A.K. Vipin).

http://dx.doi.org/10.1016/j.carbpol.2014.04.037
0144-8617/

Kouvelos, & Katsaros, 2008; Rousseau, Le Cerf, Picton, Argillier, & Muller, 2004; Smidsrød & Skjåk-Braek, 1990).

Highly dispersed carbon nanotubes (CNT), a multipurpose material were used to create a strong physical network over sodium cobalt hexacyanoferrate crystals in order to make them more stable in calcium alginate vesicle. Also the CNT helped increase the effective surface area of the composite material that improved sorption and ion exchange which directed to a meaningful removal capability (Hu, Fugetsu, Yu, & Abe, 2012).

The present work deals with the development of sodium cobalt hexacyanoferrate/calcium alginate beads modified with the dispersed carbon nanotubes. A set of experiments was done to analyze the practical application of developed adsorbent for the removal of cesium and strontium from aqueous solutions under batch and continuous flow conditions in fixed bed column. We conducted the kinetic, equilibrium and breakthrough studies. We extended our research to check the effect of pH and ionic competition on adsorption.

2. Materials and methods

2.1. Chemicals and reagents

Sodium alginate 500–600 cP, calcium chloride anhydrous, cobalt nitrate hexahydrate, sodium ferrocyanide decahydrate, cesium chloride, strontium chloride, magnesium chloride, sodium chloride, potassium chloride, aluminium chloride, hydrochloric acid and sodium hydroxide purchased from Wako Chemicals, Japan.

2.2. Preparation of sodium cobalt hexacyanoferrate (CoFC) and beads

To a solution of sodium ferrocyanide decahydrate (0.6 M in deionised water 500 mL) cobaltnitrate hexahydrate (0.6 M in deionised water 500 mL) was added slowly with mechanical stirring. The solution was mixed overnight. The colloidal product was separated via centrifugation at 10,000 rpm and the sample was washed three times in deionised water. Finally, the CoFC was allowed to drying at 80 °C for 12 h in an oven. Further chemical and physical characterisation of pure, dried CoFC was completed. Scanning electron microscopy (SEM) measurements was performed on the CoFC crystalline product by using JEOL Scanning Electron microscope, Japan. Thermo gravimetric analysis (TGA) was done on samples after their initial drying at 80 °C for 12 h. Thermal decomposition in the air was conducted over the temperature range of 30–1000 °C using SII EXSTAR 6000 TG/DTA analyzer. The FT-IR spectrum was acquired with a JASCO FT/IR-460 *plus* in the range of 4000–400 cm^{-1} by preparing the pellets with KBr. The X-ray diffraction (XRD) measurement was conducted with the help of a Rigaku RINT Ultima diffraction apparatus having Cu Kα radiation and an X-ray power of 40 kv/20 mA at a scan rate of 40 min^{-1}.

Preparation of sodium alginate solution was simple; approximately 15 g of sodium alginate weighed out and shaken well with one litre of deionised water for one day. Calcium alginate beads were prepared by slowly dropping down 1.5% (w/v) aqueous solution of sodium alginate into a beaker containing 5% (w/v) calcium chloride solution under magnetic stirring. The beads were kept stirring in the same solution about 2 h for maturation. Successively, beads were collected, and washed three times with deionised water and stored in 1% (w/v) calcium chloride solution (Veglio', Esposito, & Reverberi, 2002). We used the same methodology for making all other beads with different colloidal solution. Calcium alginate encapsulated carbon nanotubes beads were prepared by using a colloidal solution composed of 1.5% sodium alginate and 1% highly dispersed multiwalled carbon nanotubes (MWCNT). In order to make calcium alginate encapsulated CoFC beads, we used a colloidal solution having 1.5% sodium alginate and 2.5% CoFC. For calcium alginate-encapsulated CoFC beads reinforced with CNT, we dropped a solution composed of 1.5% sodium alginate, 2.5% CoFC and 1% MWCNTs into 5% calcium chloride solution. SEM and BET studies were performed on the synthesized beads that were freeze dried for maintaining the exact internal structure.

2.3. Adsorption batch studies

Collected beads were washed three times with the deionised water and air dried for 20 min at 80 °C. Beads of a known weight were added into adsorbate solutions at different concentrations in a sealable plastic tube. The solutions were shaken on a vortex shaker at 300 rpm at room temperature. The samples were collected at different time intervals and a residual ion left in solution was determined by inductively coupled plasma-atomic emission spectrometer (ICP-AES-9000, Shimadzu). The adsorption studies included the determination of important adsorption parameter such as adsorption capacity (q), these parameter can be calculated by using Eq. (1) (Sun, Yu, & Fugetsu, 2012; Yakout & Elsherif, 2010).

$$q = \frac{V(C_0 - C_e)}{m} \quad (1)$$

where C_0 and C_e are the initial and final concentrations (mg/L) of adsorbate ions in the aqueous solution, respectively, V the volume of the solution (L), and m is the weight of adsorbent (g).

2.4. Fixed bed column adsorption

We undertook a series of continuous column analyses to investigate the practical applicability of the newly prepared adsorbent. A fixed bed system was prepared with a chromatographic glass column of length 30 cm and internal diameter 1.5 cm. The column contained 40 mL of beads. Cesium and strontium solutions were passed through the column using a small pump and flow controller (supporting information Fig. S1). The column study was specifically focused on the practical feasibility of large-scale treatment of cesium and strontium contaminated water (Al-Degs, Khraisheh, Allen, & Ahmad, 2009; Vijaya & Krishnaiah, 2010).

3. Results and discussion

3.1. Characterisation of sodium cobalt hexacyanoferrate crystals

The SEM images of CoFC showed a morphology of fine nanometre sized crystals (supporting information Fig. S2A). The fine crystals are clustered together to form a lump of the material (supporting information Fig. S2B).

In TG characterisation, when CoFC is heated, one endothermic effect corresponds to a release of water molecules observed. Afterward, thermal decomposition of the rest of the molecule occurs at higher temperatures. The thermogram indicated four decomposition steps: I (30–250 °C), II (250–450 °C), III (450–650 °C) and IV (650–1000 °C) (Kunrath, Muller, & Frank, 1978). Thermo gravimetric analysis curve for the decomposition of CoFC is shown in supporting information Fig. S3.

Since the samples had been dried at 80 °C prior to analysis, the weight loss in step I was due to the release of the 1.4 water molecules (hydrated) from one molecule of CoFC. However, this water loss did not affect the crystal structure. Step II is the most crucial step because it describes the initial steps of the decomposition of the cyano group (Jukka, Mika, Juha, Markku, & Matti, 1995; Lehto, Haukka, Koskinen, & Blomberg, 1990). The decomposition is exothermic in nature and formed several intermediate products mainly $Na_3Fe(CN)_6$ and/or $Na_3Co(CN)_6$, Na_2CO_3, Fe_2O_3, Co_3O_4 and

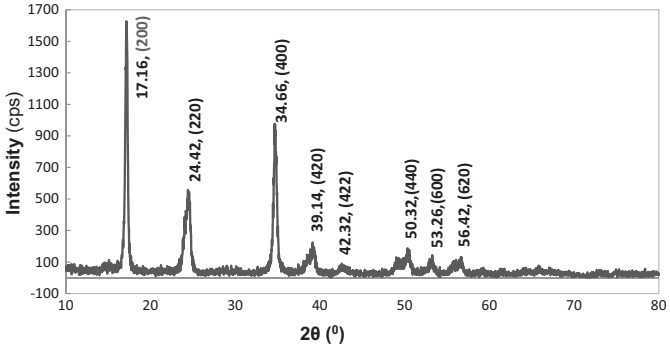

Fig. 1. XRD pattern of sodium cobalt hexacyanoferrate.

$CoFe_2O_4$. In step III, the decomposition of the intermediate products occurred. The weight loss was probably due to the evolution of gaseous compounds of carbon and nitrogen such as CO_2, NO_x and NH_3. The solid products formed in this step were Na_2CO_3, Fe_2O_3, Co_3O_4 and $CoFe_2O_4$. Above 650 °C, the final stage of the decomposition was reached, which yields Na_2CO_3/Na_2O, Fe_2O_3 and CoO as the final products (Lehto et al., 1990).

In the FT-IR spectrum of CoFC (supporting information Fig. S4), the sharp peak at 2079.85 cm^{-1} is characteristic of the Fe–CN bond, corresponding to the stretching vibration of Fe–CN. The peaks at 3339.13 and at 1612.16 cm^{-1} were characteristic of O–H stretching and H–O–H bending modes, respectively, of the interstitial water molecules. Peaks at 588.25 and 457 cm^{-1} were associated with the metal-carbon-nitrogen bending modes (Chen, 1998; Gao, Wang, Li, & Zhao, 1991; Ismail, El-Sourougy, Moneim, & Aly, 1998; Mimura, Lehto, & Harjula, 1997; Moon, Lee, & Kim, 2004).

The XRD pattern of $Na_2Co(Fe(CN)_6)\cdot 1.4H_2O$ (Fig. 1) showed characteristic diffraction peaks at 17.16°, 24.42°, 34.66°, 39.14°, 42.32°, 50.32°, 53.26° and 56.42° corresponding to the (2 0 0), (2 2 0), (4 0 0), (4 2 0), (4 2 2), (4 4 0), (6 0 0) and (6 2 0) crystal planes, respectively. This pattern confirm that CoFC having a face centered cubic structure with space group *Fm*3*m* (Farah, Shooto, Thema, & Modise, 2012; Mimura et al., 1997).

3.2. Morphological characterisation of beads

The photographs of developed CoFC encapsulated alginate beads with and without CNT reinforcement are given in supporting information Fig S5. The SEM images (Fig. 2) of freeze dried beads of CoFC encapsulated in alginate with and without CNT reinforcement showed that both types of the full sized beads were remarkably similar in size, ranging from 2.3 to 2.5 mm in diameter (Fig. 2A and E). Images of the vertical cross section of the beads (Fig. 2B and F) showed that the beads contained several porous channels. In the horizontal cross section, the shape and structure of the channels were more visible, substantiating the similar structures of the two types of beads (Fig. 2C and G). In highly magnified images of both types of beads, they appeared highly cross-linked and with immense porosity. The capacity of calcium alginate to support and stabilize the encapsulated CoFC beads is evident. During bead formation, numerous CoFC crystals aggregated together and became encapsulated in the network of calcium alginate (Fig. 2D). Reinforcement by CNT held the CoFC more strongly inside the beads by forming a physical network over CoFC crystals figure, as illustrated by Fig. 2H. Moreover, CNT help to enclose more CoFC inside each bead, which will enhance the adsorption efficiency.

While cutting the beads the wall got disturbed and lot of CNT lost Supporting information Fig. S6A. However, when we observed the undisturbed portion Fig S6B we could see CNT network, a layer of physically cross linked CNT was formed.

Surface area and porosity are important characteristics, which are capable of affecting the quality and utility of many materials. In addition, they are helpful in understanding the structure, formation and applications of materials. For this reason, it is important to determine and control them accurately. The most widely used technique for estimating surface area is the BET method (Brunauer, Emmett and Teller, 1938). The important BET parameters are given in Table 1. We could understand that CNT succeeded to enhance the beads surface area and effective pore volume. At high surface area alginate have chance to contact with more divalent ions to make the beads stronger. From the SEM and BET studies, we could confirm the importance of CNT.

3.3. Comparative study on cesium and strontium adsorption

As the primary stage of experiment, we conducted a comparative study on the adsorption capability of prepared beads. Forty beads were added to 40 mL, 200 ppm cesium solution and allowed to shake at 300 rpm. In the case of strontium, initial concentration was 100 ppm and the number beads used was 20. Adsorption efficiency was measured at different time interval. Adsorption of strontium primarily depends on the availability of alginate matrix. In that case, encapsulation decreases effective availability of sites for adsorption. However, in our study, we found that encapsulated beads showed slightly high sorption efficiency towards strontium (supporting information Fig. S7). The results indicating that a collective adsorption by both alginate and CoFC was happened. Both calcium alginate and calcium alginate encapsulated CNT beads have negligible adsorption ability towards cesium uptake. CoFC was the vital material for the adsorption of cesium ions, therefore, CoFC encapsulated alginate beads as well as Carbon nanotubes reinforced CoFC encapsulated alginate beads were very central. The effectiveness of both types of beads was depending on encapsulation efficiency. The reinforced beads have higher adsorption capacity than normal CoFC encapsulated beads even though the difference was not so big. This increase may be due to the participation of carbon nanotubes, via physical entrapment by forming a physical network inside the beads. From the results, we could understand that the CNT not only reinforcing the beads stability but also enhancing the adsorption rate in some extent.

3.4. Equilibrium isotherm models

Equilibrium can define as the state of dynamic balance between the concentration of free metal ion in the bulk solution and the amount of metal ions bound to the adsorbent matrix. Equilibrium adsorption (the ratio of the amount of metal ion adsorbed to the amount remaining in the solution) studies are very important for sorption analysis. These studies permit us to determine the adsorption isotherm that provides information regarding the sorption mechanism, surface properties, and the affinity of the sorbent (Abd El-Latif & Elkady, 2010; Foo & Hameed, 2010). In this study, we examined the relationship between adsorbed cesium and its residual concentration in aqueous solution at equilibrium by using the Langmuir and the Freundlich isotherm models.

The Langmuir isotherm is the most widely used isotherm (Ho, Porter, & Mckay, 2002) that assumes homogeneous monolayer adsorption on well defined sites, which are identical and equivalent. Each of the definite localized sites holds one molecule and possesses equal enthalpy and sorption energy. Equilibrium describes the point beyond which no further adsorption takes place. Lateral interaction between adsorbed molecules and transmigration of the adsorbate in the plane of the surface are not present.

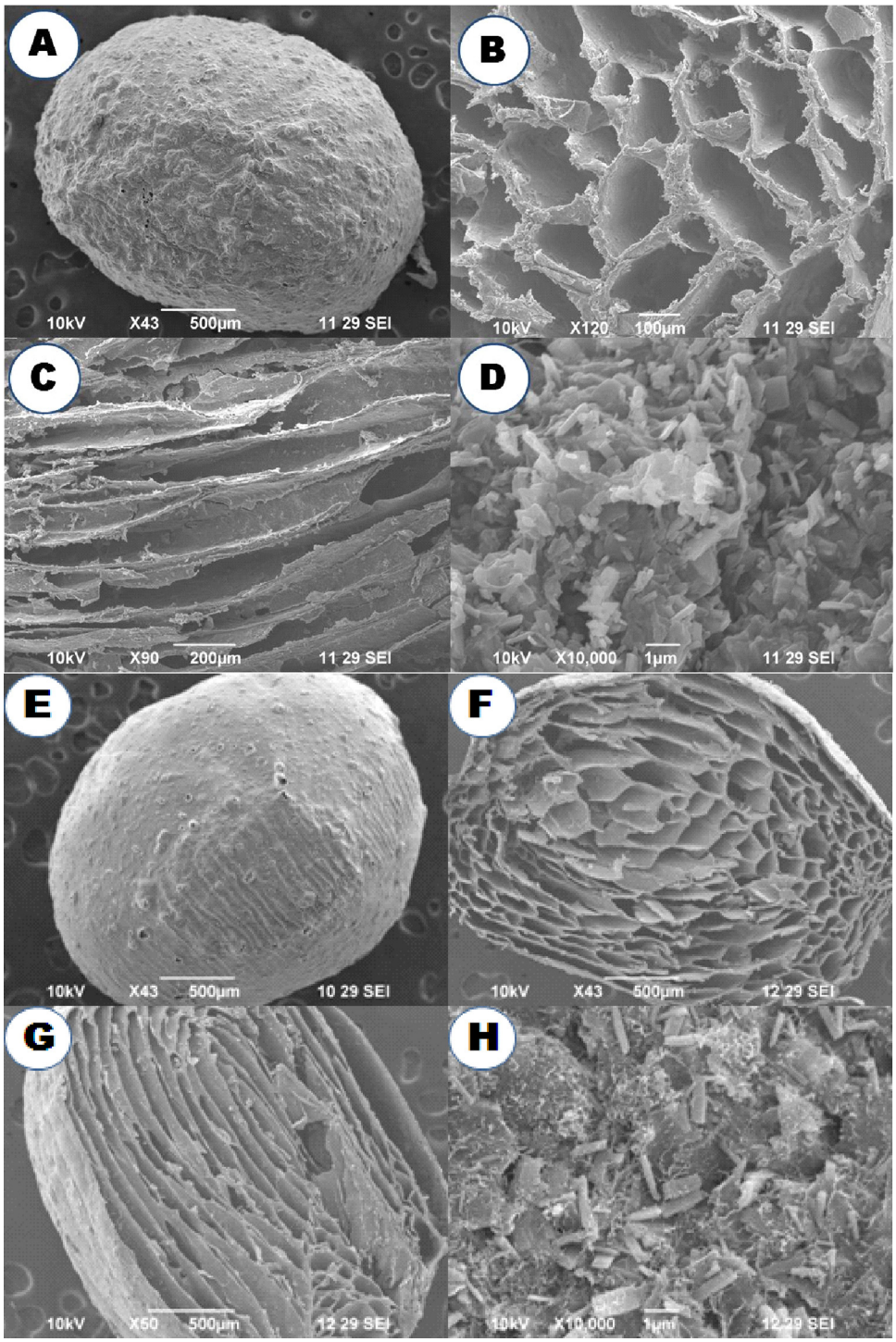

Fig. 2. SEM images of beads. Sodium cobalt hexacyanoferrate encapsulated bead without CNT: (A) whole sized, (B) vertical cross section, (C) horizontal cross section and (D) highly magnified images. Sodium cobalt hexacyanoferrate encapsulated bead with CNT: (E) whole sized, (F) vertical cross-section, (G) horizontal cross section and (H) highly magnified images.

Table 1
BET parameters of beads.

BET parameter	CoFC beads	CoFC + CNT beads	Alginate beads	Alginate + CNT beads
Surface area ($m^2\ g^{-1}$)	37.9	44.5	22.56	33.1
Pore size (nm)	25.87	38	17.03	18.12
Pore volume ($m^3\ g^{-1}$)	8.7	10.22	5.1	7.6

The non-linear form of Langmuir isotherm is represented by Eq. (2).

$$q_e = \frac{q_m K C_e}{1 + K C_e} \tag{2}$$

where q_e is the amount of adsorbate adsorbed (mg/g) at equilibrium, C_e the equilibrium concentration of the adsorbate ions (mg/L), q_m and K are Langmuir constants related to maximum adsorption capacity (mg/g) and energy of adsorption (L/mg), respectively.

The linear form of the Langmuir isotherm is represented by Eq. (3).

$$\frac{C_e}{q_e} = \frac{1}{q_m K} + \frac{C_e}{q_m} \tag{3}$$

A plot of C_e/q_e versus C_e should be a straight line with slope $1/q_m$ and intercept $1/q_m K$. The applicability of a model (goodness of fit) on experimental data can easily evaluate from the correlation coefficient (R^2) value. The significant characteristics of Langmuir isotherm can be explained by a dimensionless separation factor R_L, Eq. (4) which indicates the isotherm shape and predicts whether an adsorption is favourable or not (Günay, Arslankaya, & Tosun, 2007).

$$R_L = \frac{1}{1 + K C_0} \tag{4}$$

where C_0 is the initial adsorbate concentration (mg/L), low R_L value reflects that the adsorption is favourable. In details adsorption will be either unfavourable ($R_L > 1$), linear ($R_L = 1$), favourable ($0 < R_L < 1$) or irreversible ($R_L = 0$). In this study, the separation factor R_L was between zero and one in each case indicating the favorable adsorption.

The Freundlich isotherm is one of the first known isotherm models, which describes non-ideal and reversible adsorption. This empirical adsorption isotherm is commonly used to explain multilayer adsorption on a heterogeneous surface with no uniform distribution of adsorption heat and affinity.

The non-linear Freundlich isotherm is represented by Eq. (5).

$$q_e = K_f C_e^{1/nf} \tag{5}$$

where q_e is the equilibrium solid phase concentration (mg/g), K_f and n_f are the isotherm parameters of adsorption capacity (mg/g) and adsorption intensity, respectively; C_e is the equilibrium liquid phase concentration (mg/L).

The linear form of Freundlich isotherm can be represented as given below.

$$\ln q_e = \ln K_f + \frac{1}{nf} \ln C_e \tag{6}$$

when $\ln q_e$ plotted against $\ln C_e$, a straight line with slope $1/n_f$ and intercept $\ln K_f$ would be obtained. The value $1/n_f$ is the heterogeneous factor, describing a surface that becomes more heterogeneous as the value gets closer to zero. The Freundlich parameters such as K_f and n_f were calculated from the slope and intercept values.

In our experiment, the Langmuir R^2 value for CoFC encapsulated beads without and with CNT was high, indicating a very good mathematical fit and adsorption following the Langmuir model for both types of beads (supporting information Fig. S8).

The Langmuir parameters of q_m and K were calculated from the slope and intercept values (Table 2).

The maximum monolayer adsorption capacity of CoFC encapsulated beads with CNT slightly exceeded the value of CoFC encapsulated beads without CNTs (~8.5% higher). The presence of reinforcing CNT had no adverse effect on cesium uptake. Indeed, the CNT gave a small enhancement to adsorption of free cesium from the solution. The effectiveness of both types of beads was dependent on encapsulation of CoFC; CNT have great ability to increase the encapsulation. This slight boost in adsorption conferred by CNT may reflect a larger physical network that can entrap cesium inside the beads. Even though the adsorption efficiencies of the two types of beads were not so different, the stability of normal encapsulated bead was less as compared to CNT reinforced beads prepared at the same alginate concentration. The Freundlich correlation coefficient (R^2) values were relatively lower than for the Langmuir model in each case, suggesting poorer fit of the data. Based on the data in Table 2, we calculated the heterogeneous factor $1/n_f$ of the CoFC encapsulated beads with and without CNT. Both values fall in between zero and one, indicating that the surface of bead is heterogeneous as well as adsorption follows chemisorptions.

Table 2
Various equilibrium isotherm model parameters for sodium cobalt hexacyanoferrate encapsulated alginate beads without and with CNT.

	Cesium		Strontium	
	CoFC	CoFC + CNT	CoFC	CoFC + CNT
Langmuir				
q_m (mg/g)	121.95	133.33	71.9424	72.9927
K (L/mg)	0.048	0.023	0.197	0.06
R_L	0.095	0.18	0.076	0.20496
R^2	0.9911	0.983	0.9842	0.9814
Freundlich				
K_f	54.15	31.817	18.7	36.6
n_f	7.386	4.274	3.643	6.7659
R^2	0.8125	0.8884	0.953	0.7443

3.5. Adsorption kinetics

In solid/solution adsorption processes, kinetic studies let us assess the uptake rate performance and mechanism. For design of industrial adsorption column, the prediction of batch sorption kinetic is very essential. Various adsorption kinetic models are available to evaluate sorption kinetics. In this study, two kinetic models were used such as pseudo-first-order and pseudo-second-order models (Ho & Mckay, 2000; Ho & Mckay, 2002; Qiu, Lv, Pan, Zhang, Zhang, & Zhang, 2009).

The non-linear form of pseudo-first-order rate equation, expressed as Eq. (7) (Kumar, 2006).

$$q = q_e(1 - \exp^{-K_1 t}) \tag{7}$$

where q_e and q are the sorption capacities (mg/g) at equilibrium and at time t, respectively, and K_1 is the pseudo-first-order rate constant (L/min).

In 1995, Ho put forward a pseudo-second-order rate equation described by Eq. (8).

$$q = \frac{K_2 q_e^2 t}{1 + K_2 q_e t} \tag{8}$$

where q_e and q are the sorption capacities (mg/g) at equilibrium and at time t, respectively, and K_2 is the pseudo-second-order rate constant (g/mg min).

For predicting the optimum kinetics and to determine parameters involved in them, non-linear method was found to be better compared to linear method. Therefore, for the present study, we followed non-linear regression analysis. The correlation coefficient (R^2) determines the applicability of a model (goodness of fit) on experimental data (supporting information Fig S9). The calculated kinetic model parameters were tabulated in Table 3. The correlation coefficient (R^2) for pseudo-second-order model indicated a strong correlation than pseudo-first-order, which led us to conclude that the adsorption process followed the pseudo-second-order kinetic model. The rate-limiting step may be chemical adsorption

Table 3
Various kinetic model parameters for sodium cobalt hexacyanoferrate encapsulated alginate beads without and with CNT.

	Cesium		Strontium	
	CoFC	CoFC + CNT	CoFC	CoFC + CNT
Pseudo-first-order				
K_1 (L/min)	0.0486	0.0368	0.0106	0.011
q_e (mg/g)	96.43	102.56	60.66	63.35
R^2	0.7158	0.901	0.9661	0.9698
Pseudo-second-order				
K_2 (g/mg min)	0.0008	0.00054	0.000185	0.000185
q_e (mg/g)	103	111.30	70.15	73.011
h (mg/g min)	8.4872	6.689353	0.910389	0.986162
R^2	0.9326	0.9962	0.9966	0.9918

involving sharing or exchange of electrons; in addition, adsorption follows Langmuir isotherm (Ho & Mckay, 2000).

3.6. Mechanism of adsorption

The CoFC structure provides sufficient crystallographic position and each molecule containing two sodium ions as well. Cesium is one of the largest monovalent alkali metal ions, having suitable size that can enclose into the crystals of CoFC. The binding force such as chemical ion exchange; ion trapping as well as physical adsorption may occur. Due to the micro porosity of the beads, water can easily enter into the core of beads containing CoFC clusters. In our study, majority of the cesium was adsorbed by CoFC and the remaining part was trapped in the cross-linked alginate structure. The CNT physical network further enhanced the process by means of weak Van der Waals force of attraction. The metal binding to sparingly soluble CoFC was mainly due to the ion exchange between hydrogen and sodium ions present in the crystal lattice. Cobalt hexacyanoferrate shows a good tendency to enclose alkali metal ions during the preparation stage itself. In this experiment, $Na_4Fe(CN)_6$ was an ingredient for the production of cobalt hexacyanoferrate, leading to the generation of sodium ions incorporated crystal. Cesium and other monovalent ions can readily penetrate to the CoFC crystal lattice and easily displace sodium ions from the lattice. These assumptions were clearly justified from the isotherm studies done with Langmuir model, suggested a monolayer type adsorption. A physical adsorption onto the crystal lattice followed by strong electrostatic forces could lead to chemical adsorption as calculated from the isotherm models (Lehto et al., 1987; Mardan et al., 1999; Moon et al., 2004; Nilchi et al., 2003).

In our composite beads, alginate matrix was the key scavenger of strontium ions. Therefore, adsorption mainly depends on the available alginate content of the beads. More over contribution of CoFC need to be concerned. The adsorption mechanism of divalent ions on alginate vesicle was well known to scientists for many years. Alginate beads contain carboxylic and hydroxyl functional groups from mannuronic and guluronic acids. Those sites are protonated or deprotonated, depending on the pH of the aqueous medium. The carboxylic –COOH group or the lone pair of electrons present in oxygen might be involved in the binding of strontium. The adsorption of strontium onto alginate matrix occurs by cation exchange, primarily to carboxyl group, and hydroxyl group plays a secondary role. Hydroxyl group plays a key role not only in ion exchange but also in determining the affinity of the complex towards different metal ions. Because of small ionic radii of strontium ion than the available window of CoFC, the uptake should be lower. However, exchange at the surface of the crystals as hydrated ions is possible (Lehto, Paajanen, & Harjula, 1992). Our isotherm study verified monolayer chemisorptions, because the experimental data fit well with Langmuir isotherm model (Papageorgiou, Katsaros, Kouvelos, Nolan, Le Deit, & Kanellopulos, 2006; Papageorgiou et al., 2008).

3.7. Effect of hydrogen ion concentration (pH)

An environmental factor that can affect every adsorption experiment is hydrogen ion concentration. The pH has a unique ability to change the whole reaction chemistry and adsorption behaviour. The influence of hydrogen ion concentration is high in the case of ion exchange processes, especially for monovalent ions because of ionic competition. In this study, the effect of pH was estimated in terms of adsorption capacity (Fig. 3).

Adsorption capacity with both types of CoFC beads reached a steady maximum at pH 4. After pH 8, a sudden increase was observed in cesium adsorption. However, in the case of strontium, adsorption capacity stood steady until pH 10. Thus, the adsorption is feasible across a wide range of pH values. At low pH, ion exchange sites are mainly protonated, making them inaccessible for ion exchange. When pH values increase, the sites become available for ion exchange, which leads to higher adsorption.

3.8. Effect of ionic competition on adsorption

The adsorption of a metal ion generally depends on the competition with other ions, which are present in solution. In our study, we considered the competition of sodium, potassium, calcium and magnesium ions with the adsorption of cesium and strontium ions. In the control groups, concentrations of cesium and strontium, ions were 0.75 and 1.1 mM, respectively. Effects of competitive ions of various concentrations on adsorption are shown in Fig. 4. In the case of cesium adsorption, most of the divalent ions showed little effect, sodium ions offered a negligible competition and potassium ions showed a modest effect at higher concentrations. From the

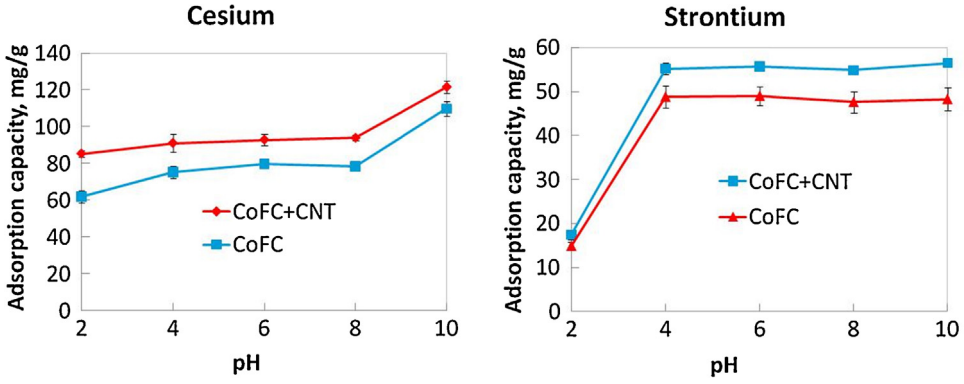

Fig. 3. Effect of pH on adsorption of cesium and strontium ions by sodium cobalt hexacyanoferrate encapsulated alginate beads with and without CNT.

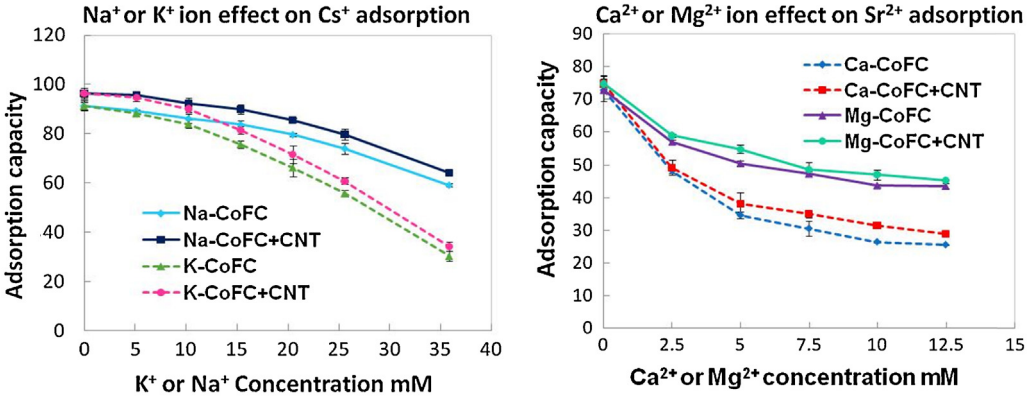

Fig. 4. Effect of competitive ions concentration on adsorption of cesium and strontium ions.

Table 4
Various parameters for the removal of cesium and strontium ions using fixed bed adsorption column.

Beads	C_i (ppm)	C_e (ppm)	b_v (mL)	m_t (mg)	q_b (mg/g)	S (%)	R_a (g/L)
Cesium							
CoFC	400	40	432	172.8	86.4	50	4.1
CoFC + CNTs	400	40	552	220.8	116.9	53	3
Strontium							
CoFC	100	10	672	58.9	29.7	50.4	2.9
CoFC + CNTs	100	10	696	61	31.3	51.3	2.84

results, we could understand that the adsorbent was highly selective towards cesium adsorption. The competition of monovalent ions on strontium adsorption was nil, but magnesium ions showed competition only at higher concentration. Even though, the adsorbent showed a high affinity towards strontium ions than other divalent ions in all concentrations, calcium ions showed an average effect on strontium adsorption compared to magnesium ions.

3.9. Fixed bed column adsorption

For both types of CoFC encapsulated beads, the breakthrough curves were obtained by plotting the ratio of effluent concentration to the influent concentration versus time (supporting information Fig. S10). The breakthrough is defined as the point when the effluent concentration from the column is about to 5–10% of the influent concentration.

The breakthrough adsorption capacity can be determined by using the following formula,

$$q_b = \left[\frac{C_i - C_e}{m}\right] bv \tag{9}$$

where C_i and C_e are the initial and breakthrough concentrations (ppm), respectively. b_v is the breakthrough volume in litres and m is the mass of the adsorbent used (g).

The other important parameters for column studies are total percentage removal, the empty bed residence time, and the adsorbent exhaustion rate.

Total percentage removal is defined as:

$$S = \frac{q_t}{m_t} \times 100 \tag{10}$$

where q_t is the adsorption capacity and m_t is amount of ions flowing through the column at time t.

$$m_t = \frac{C_0 Q t_t}{1000} \tag{11}$$

where Q is the flow rate (mL/min) and t_t is the time in minutes.

$$\text{the adsorbent exhaustion rate } (R_a) = \frac{\text{mass of adsorbent in column}}{\text{volume treated at breakthrough}} \tag{12}$$

The various parameters such as breakthrough capacity (q_b), influent concentration (C_i) and effluent concentration at breakthrough (C_e), breakthrough volume (b_v), amount of contaminant ions flowing through column at breakthrough (m_t), total percentage removal of pollutant ions (S) and adsorbent exhaustion rate (R_a) (Ghomshe, Mousavi, Soltanieh, & Kordi, 2011; Gupta Suresh, 2010; Soni, Tiwari, & Bajpai, 2012) are given in Table 4. The values gave us a conclusion that beads could perform well in continuous treatment condition. Application in industrial scale removal of cesium and strontium ions can be easily achievable. The removal capability of both cesium and strontium was relative huge that we required for solving the current problem.

4. Conclusions

We have successfully prepared durable, stable sodium cobalthexacyanoferrate encapsulated in alginate beads reinforced with highly dispersed carbon nanotubes for the removal of cesium and strontium from aqueous solutions. The CNT reinforcing beads showed high performance, having maximum monolayer adsorption of 133 mg Cs^+/g and 72 mg Sr^{2+}/g beads. The equilibrium studies were done by using two isotherm models and the goodness of mathematical fitting on adsorption model was in the order Langmuir greater than Freundlich. The adsorption kinetics studies were in the order of pseudo-second-order greater than pseudo-first-order. The uptake is monolayer chemisorptions such as ion exchange with high adsorption rate. Studies with the effect of pH confirmed that these beads could be useful over the pH range of 4–10 effectively. The performance of the beads

remained consistent even at relatively high ionic competitions. Experiments with fixed bed adsorption columns confirmed that these beads could be used for large scale treatment of cesium and strontium-contaminated water.

Acknowledgments

We would like express our sincere thanks to Hokkaido University to giving academic support. In addition, we are thankful to our laboratory members for their support.

Appendix A. Supplementary data

Supplementary material related to this article can be found, in the online version, at http://dx.doi.org/10.1016/j.carbpol.2014.04.037.

References

Abd El-Latif, M. M., & Elkady, M. F. (2010). Equilibrium isotherms for harmful ions sorption using nano zirconium vanadate ion exchanger. *Desalination*, *255*(1–3), 21–43.

Al-Degs, Y. S., Khraisheh, M. a M., Allen, S. J., & Ahmad, M. N. (2009). Adsorption characteristics of reactive dyes in columns of activated carbon. *Journal of hazardous materials*, *165*(1–3), 944–949.

Avery, S. V. (1996). Fate of caesium in the environment: Distribution between the abiotic and biotic components of aquatic and terrestrial ecosystems. *Journal of Environmental Radioactivity*, *30*(2), 139–171.

Chen, S. (1998). Characterization and electrocatalytic properties of cobalt hexacyanoferrate films. *Electrochimica Acta*, *43*(21–22), 3359–3369.

El-Kamash, A. M. (2008). Evaluation of zeolite A for the sorptive removal of Cs^{+} and Sr^{2+} ions from aqueous solutions using batch and fixed bed column operations. *Journal of Hazardous Materials*, *151*(2–3), 432–445.

Farah, A. M., Shooto, N. D., Thema, F. T., & Modise, J. S. (2012). Fabrication of Prussian blue/multi-walled carbon nanotubes modified glassy carbon electrode for electrochemical detection of hydrogen peroxide. *International Journal of Electrochemical Science*, *7*, 4302–4313.

Foo, K. Y., & Hameed, B. H. (2010). Insights into the modeling of adsorption isotherm systems. *Chemical Engineering Journal*, *156*(1), 2–10.

Fundueanu, G., Nastruzzi, C., Carpov, a, Desbrieres, J., & Rinaudo, M. (1999). Physico-chemical characterization of Ca-alginate microparticles produced with different methods. *Biomaterials*, *20*(15), 1427–1435.

Gao, Z., Wang, G., Li, P., & Zhao, Z. (1991). Electrochemical and spectroscopic studies of cobalt-hexacyanoferrate film modified electrodes. *Electrochimica Acta*, *36*(I), 147–152.

Ghomshe, S. M. T., Mousavi, S. M., Soltanieh, M., & Kordi, A. K. S. (2011). Batch and column study of haloacetic acids adsorption onto granular activated carbon. *Scientific Research and Essays*, *6*(16), 3553–3560.

Günay, A., Arslankaya, E., & Tosun, İ. (2007). Lead removal from aqueous solution by natural and pretreated clinoptilolite: Adsorption equilibrium and kinetics. *Journal of Hazardous Materials*, *146*(1–2), 362–371.

Gupta Suresh, B. B. V. (2010). Experimental investigations and theoretical modeling aspects in column studies for removal of Cr(VI) from aqueous solutions using activated tamarind seeds. *Journal of Water Resource and Protection*, *02*(08), 706–716.

Ho, Y. S., & Mckay, G. (2000). The kinetics of sorption of divalent metal ions onto Sphagnum moss peat. *Water Research*, *34*(3), 735–742.

Ho, Y. S., & Mckay, G. (2002). Application of kinetic models to the sorption of copper (II) on topPeat. *Adsorption Science and Technology*, *20*(8), 797–815.

Ho, Y. S., Porter, J. F., & Mckay, G. (2002). Equilibrium isotherm studies for the sorption of divalent metal ions onto peat: Copper, nickel and lead single component systems. *Water, Air, and Soil Pollution*, *141*, 1–33.

Hu, B., Fugetsu, B., Yu, H., & Abe, Y. (2012). Prussian blue caged in spongiform adsorbents using diatomite and carbon nanotubes for elimination of cesium. *Journal of Hazardous Materials*, *217–218*, 85–91.

Ishihara, R., Fujiwara, K., Harayama, T., Okamura, Y., Uchiyama, S., Sugiyama, M., et al. (2011). Removal of cesium using cobalt-ferrocyanide-impregnated polymer-chain-grafted fibers. *Journal of Nuclear Science and Technology*, *48*(10), 1281–1284.

Ismail, I. M., El-Sourougy, M. R., Moneim, N. A., & Aly, H. F. (1998). Preparation, characterization, and utilization of potassium nickel hexacyanoferrate for the separation of cesium and cobalt from contaminated waste water. *Journal of Radioanalytical and Nuclear Chemistry*, *237*(1–2), 97–103.

Jukka, L., Mika, P., Juha, H., Markku, R., & Matti, E. (1995). Gases evolved in the thermal decomposition of potassium cobalt hexacyanoferrate(II). *Thermochimica Acta*, *265*, 25–30.

Kumar, K. V. (2006). Linear and non-linear regression analysis for the sorption kinetics of methylene blue onto activated carbon. *Journal of hazardous materials*, *137*(3), 1538–1544.

Kunrath, J. I., Muller, C. S., & Frank, E. (1978). Thermal decomposition of potassium hexacyanoferrate(ii) trihydrate. *Journal of Thermal Analysis*, *14*, 253–264.

Lehto, J., Harjula, R., & Wallace, J. (1987). Absorption of cesium on potassium cobalt hexacyanoferrate(II). *Journal of Radioanalytical and Nuclear Chemistry*, *111*(2), 297–304.

Lehto, J., Haukka, S., Koskinen, P., & Blomberg, M. (1990). Thermal decomposition of potassium cobalt hexacyanoferrate(II). *Thermochimica Acta*, *160*, 343–347.

Lehto, J., Paajanen, A., & Harjula, R. (1992). Selectivity of potassium cobalt hexacyanoferrate(II) for alkali and alkaline earth metal ions. *Journal of Radioanalytical and Nuclear Chemistry*, *164*(1), 39–46.

Lin, Y.-B., Fugetsu, B., Terui, N., & Tanaka, S. (2005). Removal of organic compounds by alginate gel beads with entrapped activated carbon. *Journal of Hazardous Materials*, *120*(1–3), 237–241.

Mardan, A., Ajaz, R., Mehmood, A., Raza, S., & Ghaffar, A. (1999). Preparation of silica potassium cobalt hexacyanoferrate composite ion exchanger and its uptake behavior for cesium. *Separation and Purification Technology*, *16*(2), 147–158.

Mimura, H., Lehto, J., & Harjula, R. (1997). Chemical and thermal stability of potassium nickel hexacyanoferrate(II). *Journal of Nuclear Science and Technology*, *34*(6), 582–587.

Moon, J.-K., Lee, E.-H., & Kim, H.-T. (2004). Ion exchange of Cs ion in acid solution with potassium cobalt hexacyanoferrate. *Korean Journal of Chemical Engineering*, *21*(5), 1026–1031.

Nilchi, A., Malek, B., Maragheh, M. G., & Khanchi, A. (2003). Exchange properties of cyanide complexes: Part I. Ion exchange of cesium on ferrocyanides. *Journal of Radioanalytical and Nuclear Chemistry*, *258*(3), 457–462.

Papageorgiou, S. K., Katsaros, F. K., Kouvelos, E. P., Nolan, J. W., Le Deit, H., & Kanellopoulos, N. K. (2006). Heavy metal by calcium alginate beads from Laminaria digitata. *Journal of Hazardous Materials*, *137*(3), 1765–1772.

Papageorgiou, S. K., Kouvelos, E. P., & Katsaros, F. K. (2008). Calcium alginate beads from Laminaria digitata for the removal of Cu^{+2} and Cd^{+2} from dilute aqueous metal solutions. *Desalination*, *224*(1–3), 293–306.

Qiu, H., Lv, L., Pan, B., Zhang, Q., Zhang, W., & Zhang, Q. (2009). Critical review in adsorption kinetic models. *Journal of Zhejiang University SCIENCE A*, *10*(5), 716–724.

Rousseau, I., Le Cerf, D., Picton, L., Argillier, J. F., & Muller, G. (2004). Entrapment and release of sodium polystyrene sulfonate (SPS) from calcium alginate gel beads. *European Polymer Journal*, *40*(12), 2709–2715.

Smidsrød, O., & Skjåk-Braek, G. (1990). Alginate as immobilization matrix for cells. *Trends in Biotechnology*, *8*(3), 71–78.

Soni, A., Tiwari, A., & Bajpai, A. K. (2012). Adsorption of o-nitrophenol onto nano iron oxide and alginate microspheres: Batch and column studies. *African Journal of Pure and Applied Chemistry*, *6*(12), 161–173.

Sun, L., Yu, H., & Fugetsu, B. (2012). Graphene oxide adsorption enhanced by in situ reduction with sodium hydrosulfite to remove acridine orange from aqueous solution. *Journal of Hazardous Materials*, *203–204*, 101–110.

Taj, S., Muhammad, D., Chaudhry, M. A., & Mazhar, M. (2011). Lithium, rubidium and cesium ion removal using potassium iron(III) hexacyanoferrate(II) supported on polymethylmethacrylate. *Journal of Radioanalytical and Nuclear Chemistry*, *288*(1), 79–88.

Todd, T. A., Batcheller, T. A., Law, J. D., & Herbst, R. S. (2004). Cesium and strontium separation technologies literature review. In *INEEL/EXT-04-01895*. Idaho National Engineering and Environmental Laboratory.

Veglio', F., Esposito, a, & Reverberi, a. (2002). Copper adsorption on calcium alginate beads: Equilibrium pH-related models. *Hydrometallurgy*, *65*(1), 43–57.

Vijaya, Y., & Krishnaiah, A. (2010). Column adsorption and desorption studies of fluoride on perchloric acid cross-linked calcium alginate beads. *E-Journal of Chemistry*, *7*(1), 265–270.

Yakout, S. M., & Elsherif, E. (2010). Batch kinetics, isotherm and thermodynamic studies of adsorption of strontium from aqueous solutions onto low cost rice-straw based carbons. *Carbon–Science and Technology*, *1*, 144–153.